Journal of Alloys and Compounds 509 (2011) 4603–4607

Contents lists available at ScienceDirect

Journal of Alloys and Compounds

journal homepage: www.elsevier.com/locate/jallcom

# X-ray photoelectron spectroscopic study of catalyst based zinc oxide thin films

S.S. Shinde, K.Y. Rajpure*

*Electrochemical Materials Laboratory, Department of Physics, Shivaji University, Kolhapur 416004, India*

ARTICLE INFO

*Article history:*
Received 18 December 2010
Received in revised form 12 January 2011
Accepted 15 January 2011
Available online 22 January 2011

*Keywords:*
Catalyst
XPS
Chemical shifts
Bond iconicity
Auger parameter

ABSTRACT

X-ray photoelectron spectroscopy (XPS) is a powerful tool for surface and interface analysis, providing an elemental composition of surfaces and the local chemical environment of adsorbed species. The surface composition and chemical states of the F/ZnO and In/ZnO catalysts deposited using spray technique have been studied by high resolution and high sensitivity X-ray photoelectron spectroscopy. A hybrid multiline method is proposed for quantitative XPS analysis that combines the first principles approach with the experimental determination of overall response function. The chemical shifts of XPS core lines for Zn ($2P_{3/2}$, F 1s and In 3d) and Auger parameter for zinc ($\beta_{Zn}$ = 2012.6, 2011.48 eV for F/ZnO and In/ZnO, respectively) have been calculated. The results have been used to determine the bond iconicity (0.55).


## 1. Introduction

The understanding of the interaction of a catalyst's with the host surface plays a key role in a detailed description of catalytic processes. However, a spectroscopic characterization of the reacting surface under ambient conditions is challenging. While photon-in photon-out techniques can be employed at higher gas pressures, which typically show a lack of surface sensitivity. On the other hand, photon-in electron-out techniques like XPS are intrinsically more surface sensitive due to the strong interaction of (low energy) electrons with matter. Thus, the use of XPS as a tool for characterization of catalysts is an attractive tool for several apparent reasons. XPS shows a universal chemical sensitivity by probing the different core levels of the element. The surface sensitivity of XPS critically depends on the kinetic energy of the released photoelectrons and thus on the energy difference between the incoming photon and the binding energy of the core level. Low energy electrons of 50–150 eV show the smallest inelastic mean free path in a solid and thus the highest surface sensitivity [1]. Thus, XPS develops into an ultimate surface sensitive tool for characterizing the topmost layers of a material when it is operated with a tunable X-ray source at a storage ring. Synchrotron based XPS makes it feasible to ensure a low kinetic energy of the released photoelectrons for all core levels. Zinc oxide, with a direct band gap of 3.37 eV and a large exciton binding energy of 60 meV at room temperature, is attracting worldwide attention because of its potential applications in short-wavelength optoelectronic devices, such as piezoelectric sensors/actuators [2], high frequency electro-acoustic devices [3] due to their piezoelectric properties and high acoustic velocity, ultraviolet (UV) light-emitting diodes (LEDs), and laser diodes (LDs) operating at high temperatures and in harsh environments [4–9]. However, in order to develop ZnO-based optical devices, stable and high-quality n-type ZnO films are required. The major difficulty in fabrication of n-type ZnO films is the self-compensating process of doping. The electrochemical removal of the oxides present on the host surface enhances the catalytic properties of the host, indicating that the oxide(s) inhibit rather than catalyzing the evolution reaction. Since the electronic properties of the host surfaces play an important role in the catalytic activity. These arguments are based on X-ray photoelectron spectroscopy (XPS) results such as measured core level energy shifts between elements in elemental states. The measurable chemical shift is one of the main advantages of XPS technique. The chemical shift is defined as the variation in measured photoelectron (and/or Auger electron) energy arising from changes in the atomic potential, which are in turn strongly related to changes in the atomic environment. Photoelectron binding energy values are susceptible to energy referencing and/or sample electrostatic charging effects. XPS is used in this study to differentiate the species of F and In found in ZnO:F, In films. To understand how the electronic properties of the films are affected by F and In doping, XPS is used to determine positions of the valence band edge with respect to the Fermi level. Ballerini et al. [10] reported the acid–base properties of the surface of native zinc oxide layers by XPS study of adsorption of 1,2-diaminoethane. Islam et al. [11] depicted the XPS and X-ray diffraction studies of aluminum-doped zinc oxide transparent con-

* Corresponding author. Tel.: +91 231 2609435; fax: +91 231 2691533.
*E-mail address:* rajpure@yahoo.com (K.Y. Rajpure).

0925-8388/$ – see front matter © 2011 Elsevier B.V. All rights reserved.
doi:10.1016/j.jallcom.2011.01.117

ducting films. An asymmetry in Zn $2p_{3/2}$ photoelectron peaks has been observed for aluminum-doped films. The asymmetry parameters evaluated from core-electron line-shape analysis yield a value of the order of $0.04 \pm 0.01$. Amor et al. [12] studied the XPS analyses of reference and carbon dioxide plasma treated polyethylene terephthalate (PET). Significant chemical modifications were outlined in the treated PET surface in comparison with the reference one. The formation of new oxygenated groups was evidenced. These modifications heighten the level of interactions between the polymer substrate and the deposited coating. The line shape changes in the high-resolution core level spectra of carbon (C1s), oxygen (O1s), and zinc (Zn2$p_{3/2}$, Zn3p), with the progressive deposition of zinc oxide coatings.

In the present paper a two step approach for quantitative XPS analysis of doped zinc oxide catalyst is presented. In the first step the kinetic energy dependence of the detection efficiency of the spectrometer was determined for the experimental set-up using pure ZnO as a standard. The effective response function was related to the transmission function of the spectrometer via specimen dependent parameters such as refraction and reflection indices or diffraction of the photoelectrons, that need not be determined if quantitative analysis is required. In the second step the dopant surface concentrations were obtained from the first principle analysis of their XPS peaks intensities. Simultaneously the ZnO matrix peaks were used for the evaluation of the thickness of the carbon contamination over layer by the multiline treatment. Also this paper reports material characterization, viz. the chemical and Auger parameter shifts, bond ionicity of zinc oxide thin films on a glass using XPS technique.

## 2. Experimental

The binary (F/ZnO and In/ZnO) catalyst based zinc oxide thin films were deposited on ultrasonically cleaned corning glasses by chemical spray pyrolysis using aqueous solutions of analytical reagent grade zinc acetate, ammonium fluoride and indium trichloride as precursors. To realize catalysis of fluorine and indium, ammonium fluoride ($NH_4F$) and/or indium trichloride ($InCl_3$) was added in the 0.1 M zinc acetate (99.99%, A.R. Grade, Aldrich) solution. The [F]/[Zn] and [In]/[Zn] ratios calculated on at%, used in the starting solution were 5, 10, 15, 20 at% and 1, 2, 3, 4, 5 at%, respectively. Influences of fluorine and indium in zinc oxide lattice are studied using structural, optical and electrical characterization and have been reported elsewhere [13,14]. These typical optimized thin films of F:ZnO and In:ZnO were analyzed by X-ray photoelectron spectroscopy for their electronic structural analysis, compositional analysis, surface sensitivity, etc.

XPS spectra were recorded using an ESCA spectrometer (ULVAC-PHI 5600). The measurements were performed for a freshly cleaved sample surface. The energy resolution of the spectrometer was about 1 eV at pass energy 50 eV. Zn 2p, O 1s, F 1s and In 3d lines were systematically recorded. Monochromatized X-ray (Kα: 1486.61 eV) from an Al anode was used for excitation. An electron flood gun was employed to compensate for the sample charging under X-ray irradiation. The overall resolution was about 0.5 eV under our experimental conditions. The base pressure in the sample chamber was less than $6.0 \times 10^{-8}$ Pa during the measurements.

## 3. Results and discussion

### 3.1. Surface chemical analysis of the F and In based ZnO

A typical survey and detailed spectra of the F/ZnO and In/ZnO catalysts in the Zn 2p, O ls, Zn 3p, Zn 3d, F 1s, In 3d and valence regions are shown in Figs. 1–8. The observed binding energies are summarized in Table 1 for all the films investigated.

Good agreement is found between the observed BE and the literature data for ZnO [15,16]. The XPS survey spectrum is dominated by the ZnO pattern and only the 1s peak of fluorine (Fig. 1) and 3d peaks of indium (Fig. 8) are detected. The pronounced splitting of the Zn 2p spectral line into the $2p_{1/2}$ and $2p_{3/2}$ lines is observed (Fig. 2), despite the instrument operating set-up, which aimed at an improvement of the sensitivity with some sacrifice of resolution. The valence band (VB) spectra revealed the bottom of the VB, above the Zn 3d line, whereas the FWHM value of the VB was about

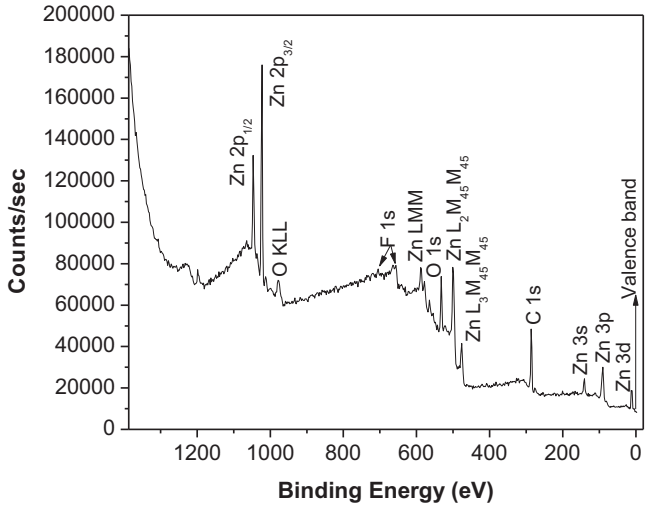


**Fig. 1.** Survey scan spectrum of the fluorine based zinc oxide (15 at% F:ZnO) thin film taken at room temperature.

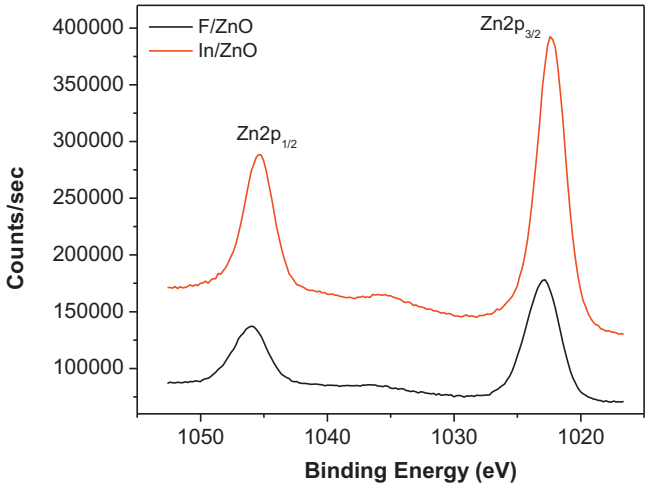


**Fig. 2.** Photoelectron spectrum of the Zn $2p_{3/2}$ and $2p_{1/2}$ region of polycrystalline 15 at% fluorine and 3 at% indium based zinc oxide thin films.

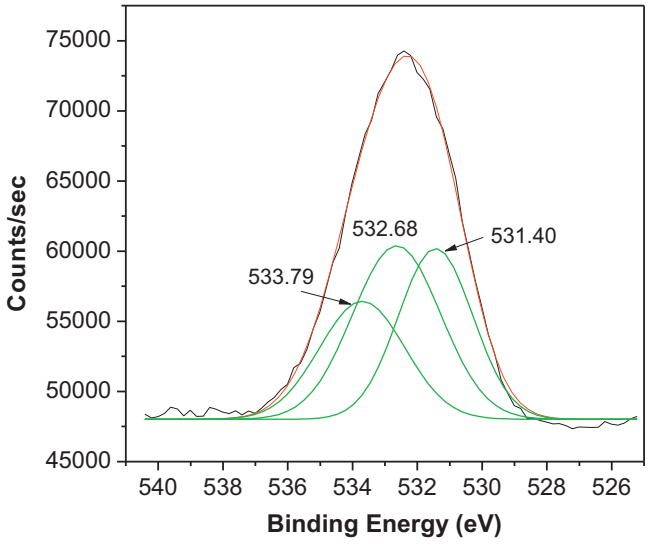


**Fig. 3.** Photoelectron spectrum of the O 1s region of 15 at% F doped ZnO catalyst.

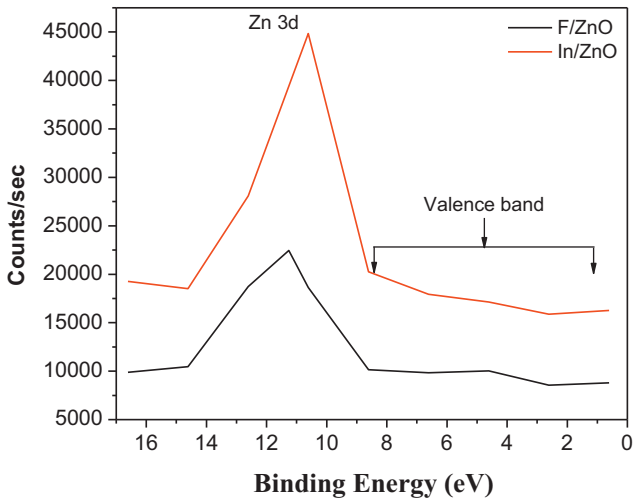


**Fig. 4.** Photoelectron spectrum of the Zn 3d and valence band region of the 15 at% F and 3 at% indium doped ZnO catalysts.

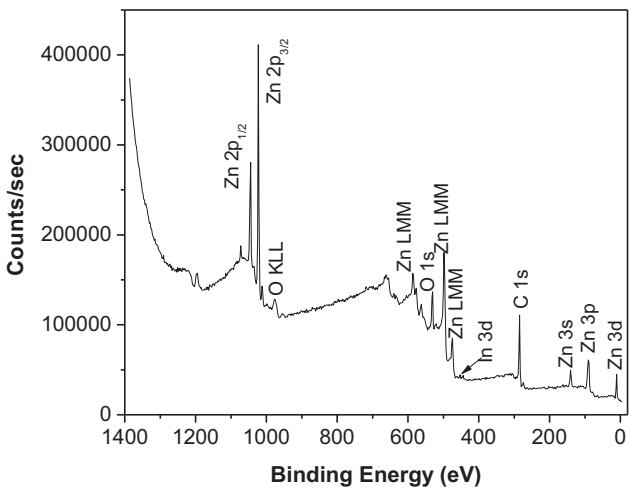


**Fig. 6.** Survey scan photoelectron spectrum of the indium based zinc oxide (3 at% In:ZnO) thin film taken at room temperature.

3.95 eV (Fig. 4).

Assuming that the photoelectron intensity reflects the density of states with little or no distortion, the density of states in the VB had maxima at 6 eV and 4 eV above Zn 3d (Fig. 4). The theory of the ZnO VB indicates that the lower binding energy portion of the VB consists mainly of O 2p and Zn 4p levels, whereas the higher BE portion of the VB has major O 2p and Zn 4s character [15]. An attempt is made to determine changes in the ZnO VB spectrum due to the presence of the F 1s and In 3d levels by comparing the VB spectra of doped and pure ZnO.

However, substraction of the VB spectrum of doped ZnO from the VB of undoped ZnO matrix did not reveal a significant intensity due to F 1s or In 3d, most probably caused by low concentrations of these elements. The higher BE peak was observed on most metal oxides but its exact origin is somewhat uncertain [17] and its assignment to hydroxyl groups [18,19], carbonates [20] or surface oxygen [21] is common. Although the O1s peak at 531.2–531.9eV was attributed to surface OH groups [18], this is unlikely to be the case for the currently studied specimens because our method of sample handling and introduction to the spectrometer prevented sample contamination by water vapor in air. We tend to attribute the O1s peak at ~532.34 eV to surface oxygen species.

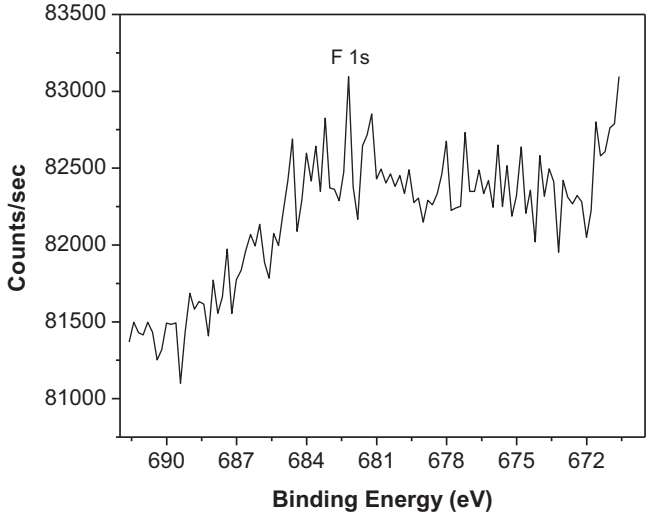


**Fig. 5.** The F 1s XPS line of the 15 at% F doped ZnO sample with Al Kα radiation.

The F 1s peak in the 15 at% F/ZnO is presented in Fig. 5. The line could be well fitted, with a single Voigt function showing the predominance of one species only. At top layers of the film or lower depths the oxygen and fluorine concentration are less compared to higher depths. This probably results due to the escape of oxygen and fluorine into atmosphere from top layers. The In 3d spectrum in the 3 at% In/ZnO showed a well doublet (Fig. 8).

It is unlikely that the incident X-ray flux can produce chemical changes directly, i.e. via simple photochemical process. The main reason for chemical decomposition is the flux of secondary electrons, either those produced inside the sample by slowing down the primary photoelectrons [22], or those coming to the sample from the surroundings [23]. Inelastic collisions can induce further valence or core electron ionizations (generating lower energy secondary electrons) or induce transitions from the valence band to the conduction band, producing freely propagating excitons [24]. As a result, solid material bathed in high energy radiation can acquire a stationary concentration of excitonic pairs, especially when irradiated with lower energy photons from Bremsstrahlung. The motion of the excitons may be terminated at impurity sites.

Generally the O 1s peak has been observed in the BE region of 529–535 eV. The peak around 529–530 eV has been attributed to lattice oxygen and the peak around 530.7–531.6 eV to oxygen in non-stoichiometric oxides in the surface region and the peak at 533 eV to a weakly bound surface oxygen. For chemisorbed $O_2$ on the metal surface the BE's are found to be in the region 530–530.9 eV, for the surface oxides and hydroxides in the region 529.6–531.0 eV and 533.3 eV, respectively. For water it is observed in the range 533.9–535.7 eV [25].

Figs. 3 and 7 show O 1s region of XPS spectra of F/ZnO and In/ZnO films. The spectrum of F/ZnO sample shows mainly O 1s peak at 532.68 eV with small shoulders at about 533.79 and 531.40 eV. The O 1s peak of In/ZnO film has peak at 532.32 eV with shoulders at 534.18 and 530.78 eV. The peak is assigned to oxygen atoms bound to Zn in ZnO while the shoulder has been assigned to the presence of moisture as its binding energy lies between 531.5 eV (OH) and 533 eV ($H_2O$) due to chemisorbed oxygen [26–28].

### 3.2. Chemical shifts and bond iconicity

Figs. 2, 5 and 8 show the expanded runs of the strongest XPS core lines Zn (2p doublet), F 1s and In (3d doublet), respectively. Fig. 2 presents the doublet lines of Zn corresponding to $2p_{3/2}$ and $2p_{1/2}$ at 1022.8 and 1045.9 eV, respectively, while Fig. 5 shows the

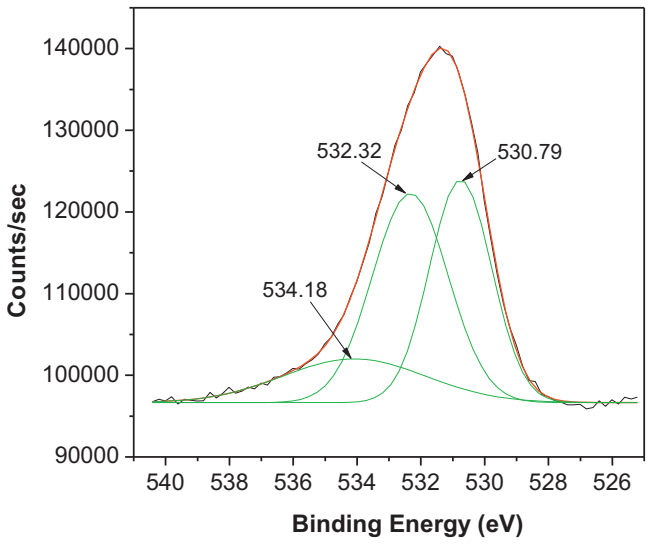


**Fig. 7.** Photoelectron spectrum of the O 1s region of the 3 at% In doped ZnO catalyst.

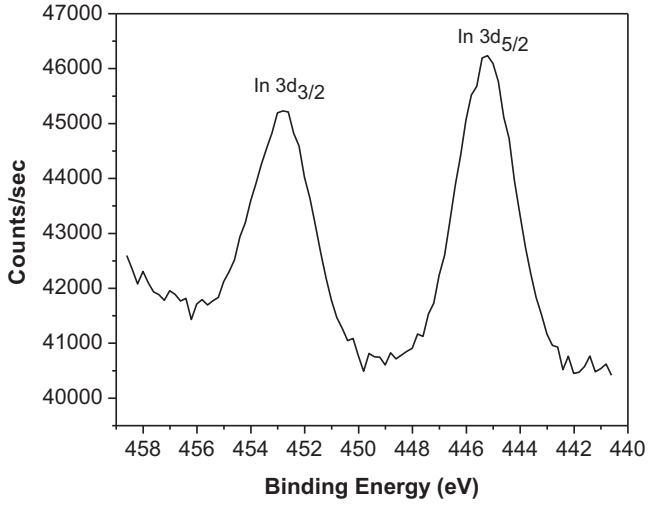


**Fig. 8.** The In $3d_{5/2}$ and $3d_{3/2}$ XPS lines of the 3 at% In doped ZnO film with Al Kα radiation.

F 1s line at 682.21 eV for F/ZnO film. The Zn ($2p_{3/2}$) line has been shifted by $\Delta E_{Zn}$ = 1.1 eV from the reported average binding energy position of 1021.7 eV for elemental zinc [26,27]. The corresponding shift for In (3d) line shown in Fig. 8, is $\Delta E_{In}$ = −0.91 eV from the reported BE position. The signs of the chemical shifts indicate electron transfer from Zn to In during the bonding process leading to a net change of the charges $\Delta q_{Zn}$ and $\Delta q_{In}$. The charge transfer can be estimated using a simple electrostatic model [27] according to which the atoms emitting photoelectrons are treated as a

**Table 1**
Binding energies (eV) for the typical 15 at% F and 3 at% In doped ZnO.

| Photoelectron | F/ZnO (eV) | In/ZnO (eV) |
|---|---|---|
| Zn $2p_{1/2}$ | 1045.9 | 1045.5 |
| Zn $2p_{3/2}$ | 1022.8 | 1022.37 |
| Zn 3p | 91.65 | 90.8 |
| Zn 3s | 139.09 | 140.05 |
| Zn 3d | 11.26 | 10.59 |
| O 1s | 532.42 | 531.42 |
| F 1s | 682.21 | – |
| In $3d_{3/2}$ | – | 452.79 |
| In $3d_{5/2}$ | – | 445.21 |

**Table 2**
Determination of the surface concentrations of F and In dopants in ZnO.

| Catalyst | Bulk F/Zn ratio | Bulk In/Zn ratio | Surface F/Zn ratio | Surface In/Zn ratio |
|---|---|---|---|---|
| F/ZnO | 0.15 | – | 0.065 | – |
| In/ZnO | – | 0.03 | – | 0.1 |

thick uniform conducting charge shell of valance electrons lying between radii $\Gamma r$ and $r$ surrounding the inner core levels (where is $r$ the atomic radius; $r_{Zn}$ = 1.31 Å, $r_{In}$ = 1.55 Å and $r_F$ = 1.33 Å). The corresponding core shifts are then given by:

$$\Delta E_x = \left(\frac{e^2}{4\pi\varepsilon_0}\right)\Delta q_x\left[\frac{A(\Gamma)}{r_x} - \frac{\alpha_s}{R}\right] \quad (1)$$

where $x$ = Zn, In, F are in the units of electronic charge $e$, $\alpha_s$, the Madelung constant for the surfaces and $R$ (1.95 Å) the nearest neighbor distance. The coefficient $A(\Gamma)$ is determined by the charge distribution which is given by:

$$A(\Gamma) = \frac{3}{2}\left(\frac{1-\Gamma^2}{1-\Gamma^3}\right) \quad (2)$$

The geometrical factor $\Gamma$ can vary between zero (for a charge sphere) and one (for charge shell).

The bond ionicity ($f_i$) has been calculated using the relation,

$$f_i = \frac{\Delta q_{Zn}}{2} = \frac{\Delta q_{In}}{3} = \Delta q_F \quad (3)$$

The bond iconicity is about $f_i$ = 0.55 and 0.30 for zinc and indium, respectively.

### 3.3. Surface composition

The atomic ratios F/Zn and In/Zn are the simplest parameters that can be determined by XPS analysis for indicating the surface stoichiometry of the doped zinc oxide catalysts. In order to convert the XPS peak areas into surface concentration a hybrid method was developed, which combines first-principle calculations with the use of a reference standard for the determination of the effective spectrometer detection function employing the multiline data treatment [8]. The X-ray flux $\Phi$ is incident at an angle $\phi$ onto the specimen. The photoelectrons originate from a layer of thickness $dz$ at a distance $z$ below the interface between a possible contamination layers. Electrons emitted at an angle $\varepsilon$ from the surface normal are detected by the spectrometer.

The analytical results presented in Table 2 are quite insensitive to the specific form of dispersion of the adventitious carbon contaminant and depend little on whether the carbon is assumed to be spread in an attenuating over layer or agglomerated in particles that cause no attenuation of the sample signals. The extent of the enrichment depends on the dopant, and for F/ZnO it is distinctly smaller than for In in In/ZnO because of penetration depth of In/Zn is large as compared to F/Zn.

The Auger peaks of Zn and O are also seen in the spectrum at 586.43, 500.5, 476.16 and 978 eV in F/ZnO and In/ZnO, respectively. An Auger transition line for Zn ($L_3M_{45}M_{45}$) is observed at BE 497.94 and 497.5 eV in F/ZnO and In/ZnO spectra. The strongest Auger line Zn ($L_3M_{45}M_{45}$) has been shifted by $\Delta E_k$ = 2.2 and 2.69 eV in F/ZnO and In/ZnO spectra from the reported average binding energy position for elemental zinc [29–31]. The sum of the binding energy $E_B$ (Zn $2p_{3/2}$) and the kinetic energy $E_k$ [Zn ($L_3M_{45}M_{45}$)] is defined as the Auger parameter $\beta_{Zn}$ for zinc [29].

$$\beta_{Zn} = E_B\left[Zn(2p_{3/2})\right] + E_k\left[Zn(L_3M_{45}M_{45})\right] \quad (4)$$

The Auger parameter can be used to compare reliably the results of different XPS studies, because it is independent of the calibration accuracy of the binding energy scale. Auger parameter (2012.6, 2011.48 eV) has been shifted by $\Delta\beta_{zn} = -1.4$, $-2.52$ for F, In/ZnO from the reported average value of 2014.0 eV for elemental zinc [30]. The Auger parameter shift is equal to the shift in the relaxation energy ($\Delta\beta_{zn} = \Delta E_R$) of a hole state in core level (e.g. Zn 2p) of the Zn atom emitting photoelectrons [31]. Thus, the corrected chemical shift ($\Delta E^c_{Zn}$) of Zn the initial state energies of Zn (2p) core level is given by,

$$\Delta E^c_{Zn} = \Delta\beta_{Zn} + \Delta E_R \quad (5)$$

Substituting the Auger parameter shift and shift in the relaxation energy, the corrected value of chemical shift has been found to be $\Delta E^c_{Zn} = +0.3$ eV instead of $\Delta E_{Zn} = +0.4$ eV. Fig. 1 shows the XPS spectra of F/ZnO and In/ZnO film on glass, for the binding energy range 0–1486 eV. The spectrum contains all the major core lines of zinc, fluorine and indium, as well as the Zn (LMM) Auger transition lines. The bond ionicity and the film composition have been estimated considering the chemical shifts and intensities of the two strongest XPS lines, namely Zn($2p_{3/2}$) and In (3d).

## 4. Conclusions

The F/ZnO and In/ZnO films deposited by spray pyrolysis has been characterized by XPS. The chemical shift of the XPS lines have been measured and used to calculate the bond ionicity of 0.55 and 0.33 for Zn and In. The bond ionicity value from XPS results is in excellent agreement with reported ionicity measurements by other experimental techniques. The analysis reveals that in the near-surface region F and In introduced into the ZnO matrix form a true solid solution with $F^-$ in substitutional (oxygen) positions and $In^{3+}$ is substituted to Zn. We have studied the actual transition of electrons in the core levels.

## Acknowledgement

The authors are very much thankful to Defence Research and Development Organization (DRDO), New Delhi, for the financial support through its Project No. ERIP/ER/0503504/M/01/1007.

## References

[1] S. Tanuma, C.J. Powell, D.R. Penn, Surf. Interface Anal. 21 (1994) 165.
[2] S. Gonzïalez-Castilla, J. Olivares, M. Clement, E. Iborra, J. Sangrador, J. Malo, J.I. Izpura, Appl. Phys. Lett. 92 (2008) 183506.
[3] Y. Satoh, T. Nishihara, T. Yokoyama, M. Ueda, T. Miyashita, Jpn. J. Appl. Phys. 44 (2005) 2883.
[4] Z.K. Tang, G.K.L. Wong, P. Yu, M. Kawasaki, A. Ohtomo, H. Koinuma, Y. Segawa, Appl. Phys. Lett. 72 (1998) 3270.
[5] D.C. Look, Mater. Sci. Eng. B 80 (2001) 383.
[6] D.K. Kim, H.B. Kim, J. Alloys Compd. 509 (2011) 421–425.
[7] R.K. Singhal, A. Samariya, Y.T. Xing, S. Kumar, S.N. Dolia, U.P. Deshpande, T. Shripathi, E.B. Saitovitch, J. Alloys Compd. 496 (2010) 324–330.
[8] S.S. Shinde, Prakash S. Patil, R.S. Gaikwad, R.S. Mane, B.N. Pawar, K.Y. Rajpure, J. Alloys Compd. 503 (2010) 416–421.
[9] X.H. Pan, Z.Z. Ye, J.Y. Huang, Y.J. Zeng, H.P. He, X.Q. Gu, L.P. Zhu, B.H. Zhao, J. Cryst. Growth 310 (2008) 1029.
[10] G. Ballerini, K. Ogle, M.G. Barthés-Labrousse, Appl. Surf. Sci. 253 (2007) 6860.
[11] M.N. Islam, T.B. Ghosh, K.L. Chopra, H.N. Acharya, Thin Solid Films 280 (1996) 20.
[12] S.B. Amor, M. Jacquet, P. Fioux, M. Nardin, Appl. Surf. Sci. 255 (2009) 5052.
[13] S.S. Shinde, P.S. Shinde, S.M. Pawar, A.V. Moholkar, C.H. Bhosale, K.Y. Rajpure, Solid State Sci. 10 (2008) 1209.
[14] S.S. Shinde, P.S. Shinde, C.H. Bhosale, K.Y. Rajpure, J. Phys. D: Appl. Phys. 41 (2008) 105109.
[15] D. Briggs, M.P. Seah (Eds.), Practical Surface Analysis by Auger and X-ray Photoelectron Spectroscopy, Wiley, New York, 1983, p. 498.
[16] S.S. Shinde, P.S. Shinde, V.G. Sathe, S.R. Barman, C.H. Bhosale, K.Y. Rajpure, J. Mol. Struct. 984 (2010) 186–193.
[17] G.D. Parks, M.J. Dreiling, J. Electron Spectrosc. Relat. Phenom. 16 (1979) 321.
[18] A. Cimino, B.A. de Angelis, G. Minelli, Surf. Interface Anal. 5 (1983) 150.
[19] F. Garbassi, J.C.J. Bart, G. Petrini, J. Electron Spectrosc. Relat. Phenom. 22 (1981) 95.
[20] A. Cimino, G. Minelli, B.A. de Angelis, J. Electron Spectrosc. Relat. Phenom. 13 (1978) 291.
[21] M.J. Dreiling, Surf. Sci. 71 (1978) 231.
[22] B.A. de Angelis, J. Electron Spectrosc. Relat. Phenom. 9 (1976) 81.
[23] J.F. McGlip, L.G. Main, J. Electron Spectrosc. Relat. Phenom. 6 (1975) 397.
[24] P. Burroughs, A. Hamnett, J.F. McGlip, A.F. Orchard, J. Chem. Soc. Faraday Trans. 71 (1975) 177.
[25] D. Brigg (Ed.), Handbook of X-ray and Ultraviolet Photoelectron Spectroscopy, Heydon, London, 1977, p. 295.
[26] J. Moulder, W.F. Stickle, P.E. Sobol, K.D. Bomben, J. Chastain, Handbook of X-ray Electron Spectroscopy, Perkin-Elmer, 1992.
[27] L. Avalle, E. Santos, E. Leiva, V.A. Macagno, Thin Solids Films 219 (1992) 7.
[28] W. Hanke, H. Ebel, M.F. Ebel, A. Jabloliski, K. Hirokawa, J. Electron Spectrasc. Relat. Phenom. 40 (1986) 241.
[29] C.D. Wagner, W.M. Riggs, L.E. Davis, J.E. Moueler, G.E. Muilenberg (Eds.), Handbook of X-ray Photoelectron Spectroscopy, Perkin-Elmer, Minnesota, 1979.
[30] S.P. Kowalczyk, R.A. Pollak, F.R. McFeeley, L. Ley, D.A. Shirley, Phys. Rev. B 8 (1973) 2387.
[31] R.B. Shalvoy, G.B. Fisher, P.J. Stiles, Phys. Rev. B 15 (1977) 1680.